

13B.7 THE CLIMATOLOGY, CONVECTIVE MODE, AND MESOSCALE ENVIRONMENT OF COOL SEASON SEVERE THUNDERSTORMS IN THE OHIO AND TENNESSEE VALLEYS, 1995-2006

Bryan T. Smith*, Jared L. Guyer, and Andrew R. Dean
NOAA/NWS/NCEP/Storm Prediction Center, Norman, OK

1. INTRODUCTION

Forecasting severe weather in the cool season (October-March) can pose a difficult challenge even for experienced severe weather forecasters. Parts of the United States, including Illinois, Indiana, Ohio, Kentucky, and Tennessee, are occasionally impacted by deadly severe weather outbreaks that occur in the cool season. According to Galway and Pearson (1981), cool season tornado outbreaks are rare but significant events. A recent noteworthy cool season outbreak was the 5 February 2008 Super Tuesday tornado outbreak in which 57 fatalities occurred (U.S. Department of Commerce, StormData 2008).

Aspects of severe weather research have evolved over the past decade. Some severe weather studies have focused on severe and tornadic thunderstorm environments (e.g., Thompson et al. 2003), others developed storm mode climatologies (Hocker and Basara 2008), and some focused on the relationship between parent storm type and severe weather reports (e.g., Trapp et al. 2005a, Gallus et al. 2008). Recent cool season severe studies (e.g., Monteverdi et al. 2003, Burke and Schultz 2004, Guyer et al. 2006, Smith et al. 2006, and Wasula et al. 2007) provided a better understanding of specific cool season severe weather events. For example, Burke and Schultz (2004) documented damaging bow echoes and derechos in the cool season months, increasing the awareness about the frequency of these destructive straight-line wind events, Guyer et al. (2006) examined cool season Gulf Coast region significant tornado environments, and Smith et al. (2006) contributed to a preliminary understanding of the relationship between cool season severe weather environments and convective mode.

Weather Surveillance Radar-1988 Doppler (WSR-88D) data began to be archived in the early to mid 1990s (Crum et al. 1993) and, until recently, radar-identified convective mode climatologies have not been possible. As a result, few studies have simultaneously compared and contrasted severe weather occurrences, severe storm convective modes, and mesoscale severe environments. The goal of this work is to comprehensively examine cool season severe weather climatology across the Ohio and Tennessee Valley region. To do this, we investigate relationships between severe reports, convective mode, and proximity environments based on severe weather ingredient-based parameters using archived Storm Prediction

Center hourly mesoanalysis data (Bothwell et al. 2002).

2. DATA AND METHODOLOGY

2.1 Severe report climatology

The 1995-2006 severe weather report dataset was gathered using the Severeplot program (Hart and Janish 2003). The cool season severe report data from the Ohio and Tennessee Valleys were then compiled and analyzed in a Geographic Information System (GIS). Using these data, we define a tornado day as a 24 hr period beginning at the first reported tornado time and a tornado outbreak (Galway 1977) as an event consisting of ten or more tornadoes beginning and ending at separations between synoptic systems. Also, corrections were made to a limited number of reports in the dataset appearing to be in temporal error, such as incorrect dates and erroneous report times. The large errors involving dates were easily corrected; corrections to smaller time errors were modified to match radar data. In addition to tornadoes, documented reports of large hail 0.75 in. (1.91 cm) or greater in diameter, severe straight-line wind gusts 50 kts (26 m s^{-1}) or convectively-induced wind damage were analyzed.

Trapp et al. (2006) highlighted apparent flaws in the severe convective wind report database. They found that a few errors, such as the underreported amount of damage, are inevitably thought to be a somewhat common limitation to the existing database. Other studies have found additional problems. These include overestimated wind speeds by human observers (Doswell et al. 2005), a largely secular (non-meteorological) number of reports over the past ten years (Weiss et al. 2002), and the dependence of report frequencies by population density and time of day, for example. These caveats associated with the severe report database are acknowledged but accepted for purposes of this study.

2.2 Convective Mode

Radar observations have revealed that storms associated with severe weather can vary from discrete supercells to narrow, long-lived and strongly-forced squall lines to single and multicellular thunderstorms. Thunderstorm longevity and intensity can vary widely, owing partly to the parent mesoscale and synoptic scale environment and degree of convective organization. The relationship between

* Corresponding author address: Bryan T. Smith
NOAA/NWS/NCEP/Storm Prediction Center, 120 David L. Boren Blvd., Suite 2300, Norman, OK 73072,
E-mail: Bryan.Smith@noaa.gov

convective mode and severe weather reports has been studied recently. For example, Trapp et al. (2005) investigated tornadic storms according to parent storm type by classifying storms as cell, quasi-linear convective system, or "other". Additionally, Gallus et al. (2008) provided preliminary data relating convective mode to severe weather report type, and Hocker and Basara (2008) spatially examined convective mode distributions over Oklahoma.

A radar dataset was compiled to document and analyze convective mode. This process involved matching severe reports to convective mode categories for reported tornadic and non-tornadic severe storms; this is designed for operational forecasting utility. Each storm is classified according to radar signatures matched to the severe storm report's location and event begin time. The Gibson Ridge (2008) radar software applications (GRlevel2, GRlevel3) and NCDC's NEXRAD viewer were used to analyze archived WSR-88D level-II or level-III single site radar data.

Convective mode was determined by identification of radar reflectivity structures (e.g., hook echo, bow echo, etc.) and velocity data (e.g., mesocyclone, rear inflow notch, etc.) to documented severe reports using single radar site data. Storms were then classified into three convective mode categories; supercell, quasi-linear convective system (QLCS), or "other", which consisted of either a multicell or single cell. Convective mode was determined using the volume scan immediately prior to reported severe event time with primary emphasis on the lowest elevation tilt (i.e. 0.5 degrees) of base reflectivity and velocity data for classifying non-supercell storms; secondary emphasis was then given to subsequent higher tilts of radar data if the lowest tilt was unavailable (e.g., range folded or improperly dealiased velocity data). If level II data were unavailable, then level III data were used. In situations when neither was available within 125 mi from the radar site or insufficient, incomplete, or no archived data was available, convective mode was not assessed.

Despite occasional radar limitations (e.g., horizon problem, aspect ratio, cone of silence) hindering the radar's ability to resolve fine-scale features, convective mode was determined for 5,967 out of 6,292 (95%) severe reports. When using a radar at large distance, it is acknowledged that the possibility of convective mode error could increase due to known radar distance limitations (e.g., indeterminate radar signatures). However, the ensuing error is thought to be negligible because convective mode, using radar data from an upwind radar site, seemed largely unaltered in most cases. In the few situations when storm mode was not apparent from radar data at large radial distances (i.e. 125-200 km), storms were not classified in order to possibly avoid misrepresenting storm type. When storms were not examined due to missing data, these cases were termed "unavailable". Severe storm events that occurred in the absence of apparent deep convection (e.g., shallow, weak reflectivity lines) or if no reflectivity was present (i.e. incorrect report data) were classified as "invalid". At times, classifying storms can

be unavoidably subjective based on defined criteria; this study's methods are similar to those employed in prior studies (e.g., Trapp et al. 2005a). Given the large sample size, it is thought that the results pertaining to counts of a particular storm mode versus another storm mode were not substantially affected due in part to the random nature of the storm dataset relative to radar locations.

2.2.1 Supercell

Supercell documentation was completed by examining azimuthal shear values through multiple tilts and volume scans of radar velocity data and comparing the values to mesocyclone nomograms in order to determine whether a given storm contains a deep persistent mesocyclone (i.e. a supercell according to Doswell 1996). For the present study, the term "supercell" is defined as a storm that is associated with radar velocity data that meets or exceeds mesocyclone nomogram (1 to 3.5 nautical mile) criteria (Andra 1997) for at least 10 minutes or 3 volume scans. The 1.85 km nomogram was used to try to identify the smaller spectrum of supercell storms such as mini-supercells (e.g., Davies 1993, Kennedy et al. 1993, Burgess et al. 1995). On rare occasions, supercells weakened for a period longer than 15 minutes and assumed more single cell characteristics (i.e., non-mesocyclone criteria) and then strengthened at a later time. These cyclic storms were classified as a single supercell storm rather than two different supercells. Characterizing storms in the supercell class was designed with operational relevancy in mind, particularly in a warning setting. While variable criteria exist to define persistence (e.g., 10-29 min), operational experience guided this decision, with an emphasis toward better understanding the convective mode spectrum and transitory nature of supercell structures.

2.2.1a Supercell Morphology

Supercells were categorized as discrete or embedded within a line, based upon the radar reflectivity. A discrete supercell was defined as being isolated from any quasi-linear region of ≥ 40 dBZ reflectivity or it was located on the southern end of a convective line. An embedded supercell was defined as a supercell storm located within a quasi-linear area of continuous reflectivity at the lowest volume scan ≥ 40 dBZ that extends over a distance greater than 50 km. Storm reports were associated with an embedded supercell as long as a distinct mesocyclone originating from a supercell was evident on radar and juxtaposed in time and place with the severe report. For example, if a tornado report occurred around the time of a supercell-QLCS merger, then mode was determined based on the feature (e.g., supercell mesocyclone, book-end vortex, etc.) that was co-located with the tornado at touchdown time.

2.2.2 QLCS

A convective system termed QLCS (Trapp et al. 2005a) requires a continuous area of reflectivity greater than 40 dBZ at the lowest elevation tilt and over a distance greater than 50 km in length with an aspect ratio of at least 3:1.

2.2.3 Other (Single Cell and Multicell)

A storm appearing discrete with regard to reflectivity but without a radar detectable mesocyclone was classified as a single cell. Inevitably, there may have been a few cases classified as single cell due to radar sampling and range limitations, which can reduce the radar's ability to resolve small and/or distant mesocyclones (Grant and Prentice 1996). This situation, however, appears to be relatively rare, based on examination of the entire dataset. Multicells have been defined for this study's purposes as an ordinary or organized group of cells within a line not achieving QLCS criteria or a small cluster of relatively disorganized thunderstorms with relatively high reflectivity (i.e. 40 dBZ and greater) values.

2.3 GIS-based supercell analyses

Geographic Information System (GIS) tools have enabled researchers to construct robust meteorological databases (e.g., Hocker and Basara 2008, Smith 2006) in a database management setting and sort information based on attributes. The GIS portion of this study followed a similar methodology to Hocker and Basara (2008) in order to analyze supercell frequency in an attribute and spatial environment. This portion of the study used radar viewing software to examine level-II and level-III radar data to identify supercells based on previously developed radar mesocyclone criteria. Supercell location tracking was recorded by using the latitude/longitude coordinate pair at the point location where the velocity couplet at lowest tilt or forward flank downdraft and the rear flank downdraft region coincided. Supercell start and end points were determined by the time mesocyclone criteria commenced and ceased, respectively. At supercell-identified point locations, attribute data were recorded at roughly ten minute intervals including stormID, latitude/longitude coordinates, date, time, supercell morphology, supercell demise, and a listing of associated severe storm reports. From these data, a supercell climatology was developed that spans environments from 41 distinct weather systems and 48 days. Valuable information such as supercell longevity, distance traveled, morphology, and whether the supercell was tornadic or non-tornadic was tallied from the supercell database. The data were then imported into ArcGIS and geocoded as point location features. A point-to-line vector data tool was used to chronologically concatenate the point features into line segments denoting supercell tracks (Fig. 1). Severe reports associated with their parent supercells were exclusively joined to their parent supercells in a GIS database

setting (Fig. 2). This enabled supercell queries based on information such as convective morphology, the severe database, and the environment. Query examples include but are not limited to the following: non-tornadic, tornadic, weakly tornadic, significantly tornadic, discrete, mixed-mode, and embedded. A few examples of more complex, intensive queries such as long-lived discrete significantly tornadic, short-lived discrete non-tornadic, etc. can be examined in an attempt to analyze atmospheric environments in a multitude of ways.

2.4 Mesoscale environment

2.4.1 Severe reports

Archived SPC mesoanalysis data (Bothwell et al. 2002), were utilized to further examine cool season (October-March) severe weather environments by investigating severe report based environments during the period starting in January 2003 and ending March 2006. Following methods used in Dean et al. (2006), a preliminary severe weather environment database was developed. Severe weather ingredient-based parameters such as MLCAPE, 0-6 km shear, etc. were then assigned to documented severe reports by linking each report to a grid point in the environment data, resulting in a severe report-dependent environment database.

According to an idealized modeling study by McCaul and Weisman (2001), differences between atmospheric profiles result in changes to storm intensity and morphology, and these changes tend to become more apparent in small convective available potential energy (CAPE) regimes. Schneider et al. (2006) indicate that strong shear/low instability regimes are disproportionately more common in the cool season over the region from the Ohio Valley into the Southeastern States.

2.4.2 Supercells

With spatial and temporal aspects inherent to supercells, environmental information can be extracted and analyzed over time and space using recorded latitude/longitude coordinates. This permits points along a supercell's path to be exclusively joined to the nearest hourly mesoanalysis gridpoint value. Using a 40 km grid, the first supercell latitude/longitude pair to enter a grid box was assigned the environmental data from that box. This was done to avoid duplicating environmental information from multiple supercell points within the same grid box as the supercell traveled through the analysis grid box. Severe weather ingredient-based parameters were then assigned to documented supercells, resulting in a moderately high spatial/temporal resolution supercell environment database. Multiple supercell queries were then applied based on reported severe weather type (i.e. non-tornadic, weakly tornadic, significantly tornadic),

morphology (i.e. discrete versus embedded), duration (i.e. short-lived versus long-lived), etc.

3. RESULTS

3.1 Severe report climatology

There were 6,292 documented severe weather reports that occurred within the Ohio/Tennessee Valley region during the eleven-year cool season period. The severe reports are spatially depicted in Fig. 3 and consist of 312 tornado reports, 1,931 hail reports, and 4,049 convective wind reports. The tornadoes occurred in 53 days and had the following damage ratings: F0: 96, F1: 107, F2: 76, F3: 27, and F4: 6. As a result, significant tornadoes (F2 or greater) accounted for 35 percent of the tornadoes. There were eight tornado outbreaks during the period and these tornado outbreaks included 200 of the 312 tornadoes (64 percent) and 83 of 109 significant tornadoes (76 percent). This finding suggests the cool season tornado outbreak threat is relatively infrequent, but potentially dangerous and destructive. Additionally, the sample included 1,931 large hail reports and 4,049 convective wind reports. Using the Storm Prediction Center's classification of significant hail, (hail diameter ≥ 2 in. or 5 cm) and significant wind reports (wind gusts ≥ 65 kts or 33 m s^{-1}) resulted in 30 significant hail and 245 significant wind reports. Cool season severe report counts revealed that March and November have the highest report frequency compared to other months (Fig. 4). Examining tornado reports by month demonstrates that, during the cool season, November had the highest tornado count while December had the lowest (not shown). The distribution of severe reports with respect to time of occurrence shows a diurnal trend to severe reports (Fig. 5 and 6). The data shows a relatively sharp increase in reports during the early to mid-afternoon hours when severe weather is typically near its peak. A slower decreasing trend is exhibited in the late evening to early overnight hours. These data may be indicating a climatological signal that a severe weather event typically peaks in the late afternoon hours and tends to linger through the evening hours before gradually waning during the late overnight hours.

3.2 Convective mode

Radar data were available and analyzed for 310 of 312 (99%) tornadoes, 1,841 of 1,931 (95%) hail reports, and 3,816 of 4,049 (94%) wind reports. The tornado, hail, and wind counts were then grouped by convective mode (Figs. 7-10). By examining the report distributions among the three modes, it is seen that QLCS's are responsible for 62% of the analyzed severe reports (3,695 of 5967), with severe wind reports overwhelmingly associated with QLCS. Tornadoes were found to be most common with supercells (56 percent) and more than three-fourths of significant tornadoes (77 percent) were produced by supercells (Figs. 11-12). Large hail tended to occur most frequently with single cells and multicells. However,

most significant hail reports originated from supercells. Significant wind reports occurred most frequently with QLCS, but supercells tended to have the highest percentage of significant wind reports when considered as a fraction of total wind reports by mode.

Tornadoes were most responsible for injuries (926 out of 928 occurrences) and the only known direct cause of deaths (68) from severe thunderstorms during this period. There were 236 supercells that affected the Ohio/Tennessee Valley region and 88 were tornadic (37 percent), resulting in supercells being the most prolific and efficient tornado producers. Also, 38 of the 190 (20 percent) severe QLCS were tornadic, producing 117 tornadoes. It should be noted that comparing the aforementioned convective mode tornado percentages can be misleading. Because of the large spatial and temporal scales associated with QLCS, this mode appears to be relatively less efficient in producing tornadoes given their larger size compared to supercells.

The diurnal trends of supercell and QLCS tornado reports were also examined (Fig. 13). Each severe report type displayed a tendency to be associated with the diurnal cycle. Supercell tornadoes were overwhelmingly favored during the 2200-0400 UTC period. A sudden peak of supercell tornadoes occurs in the 2200-0300 UTC period, with most tornadoes (94 of 170) disproportionately associated with four tornado outbreaks. However, QLCS tornadoes occurred generally as often as supercellular tornadoes between 0400-2100 UTC, which covers the overnight hours into the mid-afternoon. Only QLCS tornadoes exhibited a signal of having a modest threat remain into the late overnight and morning hours, when the overall tornado threat is typically at a minimum.

Supercell morphology was also examined at the time of tornado occurrence. It was found that 119 tornadoes were associated with 60 discrete supercells whereas 55 tornadoes were produced by 33 embedded supercells. Although the mode to tornado ratio is slightly higher for discrete supercells compared to embedded supercells, both modes were clearly associated with the frequent production of tornadoes.

3.2a Supercell attributes

During the eleven-year study period, 236 storms were identified as supercells and they occurred during 41 separate events yielding spatial and attribute information about each storm. Eight supercells exhibited a substantial cyclic nature during their lifetimes in which mesocyclone criteria was not evident in radar data for a period longer than 15 minutes. As a result, 244 supercell segments were catalogued. Despite the ability to examine radar in which a large majority of supercells existed during the study period, it is acknowledged that the total count of supercells (i.e. 244 segments / 236 supercells) and

associated supercell findings do not fully represent the entire cool season supercell climatology in the Ohio/Tennessee Valley region.

Trapp et al. (2005b) examined the WSR-88D Mesocyclone Detection Algorithm (MDA) (Stumpf et al. 1998). The MDA is a radar-based algorithm that detects deep (1-3 km) circulations in or around a thunderstorm. They found only 26 percent of the MDAs to be associated with tornadoes. However, they did not categorize convective mode. Using the approach in section 2.2.1, 88 tornadic supercells (89 segments) out of 236 supercells (244 segments) produced 218 tornadoes that occurred within or from supercells that tracked into the Ohio/Tennessee Valley region during the 1995-2006 cool season period. More than one-third (37%) of the supercells were tornadic, slightly higher than what was found in Trapp et al. (2005b). This may be partly the result of a different supercell identification technique used in the present study, as well as the majority of tornadoes being associated with tornado outbreaks.

Supercell longevity appears to be a characteristic that shows some discrimination between tornadic and non-tornadic supercells (Fig. 14). Tornadic supercell segments on average persisted more than twice as long as non-tornadic segments. The average distance traveled by tornadic supercell segments (89) for 88 different supercells was 170 km (106 mi) with a mean west-southwest to east-northeast motion. In contrast, non-tornadic supercell segment average distance was 81 km (51 miles). A direct correspondence between supercell longevity and path length appears valid given their high linear correlation (0.973).

Supercell tornadoes were found to travel a mean distance of 9.8 km (6.1 mi). Because supercell tornadoes on average are more intense and damaging, they were chosen to be more thoroughly analyzed compared to tornadoes produced by other storm modes. Thus, the following question was asked: "what is the percentage of supercell tornado distance compared to distance traveled by 1) all supercell segments and 2) tornadic supercell segments?" The sums of the total distance of all supercell segments is 27,845 km (17,302 mi) and tornadic supercell segments is 15,324 km (9522 mi), which were compared to supercell tornado path length 1708 km (1061 mi). The result is the average supercell tornado path length is 6.1 and 11.1 % of the average supercell and tornadic supercell path lengths, respectively. It appears that the Ohio/Tennessee Valley cool season supercell tornado path length is rather short compared to the path length of the tornado-spawning supercell itself. This confirms that the relationship between supercells and tornado generation is complex, and factors such as the mesoscale environment must also be examined.

3.3 Mesoscale environments

3.3.1 Severe reports

Severe environments were examined during the cool season from January 2003 - March 2006 due to data availability of archived SPC hourly mesoanalysis data (Bothwell et al. 2002). There were 1,924 40 km grid hours examined over a 57 day period. Ingredients-based severe weather parameters were collected for each severe report, this likely resulted in some duplication of environmental data because of instances in which multiple severe reports were assigned to the same grid box. Environmental data were stratified into tornado and severe hail/wind classes, and into convective mode and severe classes.

Results show severe weather is more likely with an unusually moist/unstable airmass during the cool season, typically within a highly sheared environment through a deep layer. However, the dataset illustrates relatively subtle differences amongst traditional instability/shear parameters with respect to discriminating between convective modes and/or report types during the cool season. Supercell tornadoes tend to be associated with substantially higher amounts of moisture and instability as compared to QLCS tornado cases. However, there are noticeable differences in sample sizes, and the relatively small QLCS sample becomes evident with the QLCS median values being skewed (upward) within the "box". The median 100mb MLCAPE value for supercell tornadoes was 1067 J kg^{-1} , while the QLCS tornado MLCAPE median was 534 J kg^{-1} (Fig 15). There is no interquartile overlap between the MLCAPE and SBCAPE distribution pairs. This suggests a shallow cool/dry surface based layer in surface data, which may be partly explained by RUC model "blend" in the hourly mesoanalysis grid boxes. Each set of tornado cases (supercell and QLCS) were typically associated with surface dewpoints of 58-64 °F (not shown). Median values for mid level lapse rates (700-500 mb) were found to be 6.8 C km^{-1} for supercell tornadoes versus 6.1 C km^{-1} for QLCS tornadoes, consistent with the greater CAPE associated with the supercell tornadoes.

Kinematic fields such as deep layer shear exhibited little if any discrimination ability for supercell tornadoes and QLCS tornadoes, with the median 0-6 km AGL shear value for each around 59 kts (Fig. 16). Similarly, there is little difference appearing to exist in low level shear (0-1 km and 0-3 km) between QLCS tornado environments and supercell tornado environments, indicating that strong vertical shear is common to both supercell and QLCS tornado environments. This is consistent with the findings of Evans and Doswell (2001). There was modest variability in effective SRH and MLCAPE between supercell tornadoes and supercell hail/wind environments (Fig. 17) with the tornado distributions exhibiting somewhat higher values compared to the hail/wind values.

3.3.2 Supercells

339 grid hours were analyzed covering 14 weather systems over 17 environment days. Key ingredients-based severe weather parameters were collected for each separate grid hour during a supercell lifetime. Supercells were categorized by tornado F-scale during their lifetime in order to examine environmental clues that may be related to a supercell's ability to produce an F2 or greater tornado versus a supercell that does not produce a tornado.

Sufficiently large variations were found among the mesoscale parameter space indicating that some parameters discriminate between supercell classes (i.e. non-tornadic, weakly tornadic, significantly tornadic), as has been shown in previous studies (e.g., Thompson et al. 2003). The Mixed Layer CAPE distributions are substantially different for the significant tornado and null tornado supercell classes with no interquartile overlap (Fig 18). Overall, cool season surface-based supercell environments are largely characterized as weakly to moderately unstable (i.e. 400 - 1300 J kg⁻¹ MLCAPE). Surface dewpoint exhibited some slight tendency for higher values in the significant tornado class versus the other two classes (Fig. 19), whereas precipitable water exhibited slight disparity between the significant tornado and non-tornado supercell classes (Fig. 20). Effective storm relative helicity exhibits discrimination ability between null and tornadic classes (Fig 21). Two composite indices, the supercell composite parameter and significant tornado parameter, using mixed layer convective inhibition (Thompson et al. 2003) also show some ability to distinguish between the three supercell classes (Figs. 22-23). Other parameters such as 0-3 km CAPE, LCL, LFC, and deep layer shear showed little to no discriminatory ability among the supercell classes (not shown).

4. SUMMARY AND CONCLUSIONS

This study's purpose is to contribute to improvements in severe weather forecasting over the Ohio and Tennessee Valleys during the cool season by simultaneously examining three severe weather components—severe reports, convective mode of severe storms, and cool season mesoscale environments associated with severe reports—and incorporating them into a detailed cool season severe weather climatology. This research is designed to increase awareness of cool season severe storm frequency and introduces a comprehensive approach to examining severe weather climatology. To accomplish this, characteristics of cool season severe weather were identified and investigated to determine which traits might be more conducive or inhibitive of severe weather.

It was found that severe wind reports resulting from QLCS's are the most common severe weather type during the Ohio and Tennessee Valley cool season. Supercells accounted for 56 percent of the tornadoes, but were associated with 77 percent of the significant tornadoes. Not surprisingly, tornado occurrence was

most frequent during tornado outbreaks (10 or more tornadoes), in which the majority of significant tornadoes occurred. As a result, one can infer most of the significant tornadoes within this region during the cool season are caused by supercells, and not QLCS's, in tornado outbreaks. While one in five severe QLCS produced tornadoes, it appears the significant tornado threat is substantially lower with QLCS's compared to discrete or embedded supercells. Figure 7 shows 56% of tornadoes occur with supercells and 38% occur in QLCS. However, for weak tornadoes (F0-F1), Fig. 11 shows they are evenly distributed between supercells and QLCS. In summary, the data indicate both supercells and QLCS contain non-trivial threats of tornadoes and QLCS tornado threats should not be downplayed.

Thirty-seven percent of the supercells examined in this study produced tornadoes. In analyzing cool season supercell characteristics, they favor a west-southwest to east-northeast mean motion around 40 kts (20 ms⁻¹). It was also found that on average, supercell and tornadic supercell path lengths were considerably longer than tornado path lengths. This illustrates the challenges in identifying tornado potential based on radar indications of mesocyclone existence.

Acknowledgements

This work benefitted from discussions with several NWS colleagues, including a careful review by Steven Weiss (SPC) and Ariel Cohen (NHC). We thank James Hocker (Univ. of Oklahoma) for providing helpful information regarding a GIS-meteorology database and Dr. Petra Zimmermann (Ball State Univ.) for providing valuable input during the early part of this study. NWSFO Norman provided access to GIS software and the SPC Science Support Branch also provided beneficial computing resources.

6. REFERENCES

- Andra, D. L., 1997: The origin and evolution of the WSR-88D mesocyclone recognition nomogram. Preprints, *28th Conf. on Radar Meteor.*, Austin, TX, Amer. Meteor. Soc., 364–365.
- Bothwell, P. D., J. A. Hart, and R. L. Thompson, 2002: An integrated three-dimensional objective analysis scheme in use at the Storm Prediction Center. Preprints, *21st Conf. on Severe Local Storms*, San Antonio, TX, Amer. Meteor. Soc., J117–J120.
- Bunkers, M. J., B. A. Klimowski, J. W. Zeitler, R. L. Thompson, and M. L. Weisman, 2000: Predicting supercell motion using a new hodograph technique. *Wea. Forecasting* **15**, 61–79.

- Burgess, D. W., R. L. Lee, S. S. Parker, S. J. Keighton, and D. L. Floyd, 1995: A study of mini supercells observed by WSR-88D radars. Preprints, *27th Conf. on Radar Meteorology*, Vail, CO, Amer. Meteor. Soc., 4-6.
- Burke, P. C. and D. M. Schultz, 2004: A 4-yr climatology of cold-season bow echoes over the continental United States. *Wea. Forecasting*, **19**, 1061-1074.
- Crum, T. D., R. L. Alberty, and D. W. Burgess, 1993: Recording, archiving, and using WSR-88D data. *Bull. Amer. Meteor. Soc.*, **74**, 645-653.
- Davies, J. M., 1993: Small tornadic supercells in the central plains. Preprints, *17th Conf. Severe Local Storms*, St. Louis, MO, Amer. Meteor. Soc., 305-309.
- Dean, A. R., R. S. Schneider, and J. T. Schaefer, 2006: Development of a comprehensive severe weather forecast Verification system at the Storm Prediction Center. Preprints, *23rd Conf. Severe Local Storms*, St. Louis MO, Amer. Meteor. Soc., CD-ROM.
- Doswell, C.A. III, H.E. Brooks, and M.P. Kay, 2005: Climatological estimates of daily nontornadic severe thunderstorm probability for the United States. *Wea. Forecasting*, **20**, 577-595.
- Doswell, C. A. III, 1996: What is a supercell? Preprints, *18th Conf. Severe Local Storms*, San Francisco, CA, Amer. Meteor. Soc., p. 641.
- Evans, J. S. and C. A. Doswell III, 2001: Examination of derecho environments using proximity soundings. *Wea. Forecasting*, **16**, 329-342.
- Gallus, W. A., N. A. Snook, and E. V. Johnson, 2008: Spring and Summer severe weather reports over the Midwest as a function of convective mode: A preliminary study. *Wea. Forecasting*, **23**, 101-113.
- Galway, J. G., 1977: Some climatological aspects of tornado outbreaks. *Mon. Wea. Rev.*, **105**, 477-484.
- Galway, J. G., and A. Pearson, 1981: Winter tornado outbreaks. *Mon. Wea. Rev.*, **109**, 1072-1080.
- Gibson Ridge Software, 2008: [Available at <http://www.grlevelx.com>].
- Grant, B. N. and R. Prentice, 1996: Mesocyclone characteristics of mini supercell thunderstorms. Preprints, *15th Conf. on Wea. Analysis and Forecasting*, Norfolk, VA., Amer. Meteor. Soc., 362-365.
- Guyer, J. L., D. A. Imy, A. Kis, and K. Venable, 2006: Cool season significant (F2-F5) tornadoes in the Gulf Coast states. Preprints, *23rd Conf. Severe Local Storms*, St. Louis, MO, Amer. Meteor. Soc., CD-ROM.
- Hart, J. A., and P. R. Janish, 2003: SeverePlot v2.2. Historical severe weather report database. National Weather Service Storm Prediction Center, Norman, OK. [Available Online: <http://www.spc.noaa.gov/software/svrplot2/>].
- Hocker, J. E. and J. B. Basara, 2008: A Geographic Information Systems-based analysis of supercells across Oklahoma from 1994 to 2003. *J. Appl. Meteor. & Climo.*, **47**, 1518-1538.
- Kennedy, P. C., N. E. Westcott, and R. W. Scott, 1993: Single-Doppler radar observations of a mini-supercell tornadic thunderstorm. *Mon. Wea. Rev.*, **121**, 1860-1870.
- McCaul, E. W. Jr. and M. L. Weisman, 2001: The sensitivity of simulated supercell structure and intensity to variations in the shapes of environmental buoyancy and shear profiles. *Mon. Wea. Rev.* **129**, 664-687.
- Monteverdi, J. P., C. A. Doswell III, and G.S. Lipari, 2003: Shear parameter thresholds for forecasting tornadic thunderstorms in northern and central California. *Wea. Forecasting*, **18**, 357-370.
- NCDC Nexrad Data Inventory, 2008: National Oceanic and Atmospheric Administration, National Climatic Data Center, Asheville, NC. <<http://www.ncdc.noaa.gov/nexradinv/>>.
- Schneider, R.S., A.R. Dean, S.J. Weiss, and P.D. Bothwell, 2006: Analysis of estimated environments for 2004 and 2005 severe convective storm reports. Preprints, *23rd Conf. Severe Local Storms*, St. Louis MO, Amer. Meteor. Soc., CD-ROM.
- Smith, B. T., 2006: SVRGIS: Geographic Information System (GIS) graphical database of tornado, large hail, and damaging wind reports in the United States (1950-2005). Preprints, *23rd Conf. Severe Local Storms*, St. Louis, MO, Amer. Meteor. Soc., CD-ROM.
- Smith, B. T., C. Omitt, and J. L. Guyer, 2006: Characteristics of cool season severe environments in the Ohio Valley (1995-2006). Preprints, *23rd Conf. Severe Local Storms*, St. Louis, MO, Amer. Meteor. Soc., CD-ROM.
- Stumpf, G. J., A. Witt, E. D. Mitchell, P. L. Spencer, J.T. Johnson, M. D. Eilts, K. W. Thomas, and D. W. Burgess, 1998: The National Severe Storms Laboratory mesocyclone detection algorithm for the WSR-88D. *Wea. Forecasting*, **13**, 304-326.
- Thompson, R. L., R. Edwards, J.A. Hart, K.L. Elmore and P.M. Markowski, 2003: Close proximity soundings within supercell environments obtained from the Rapid Update Cycle. *Wea. Forecasting*, **18**, 1243-1261.
- Thompson, R.L, C. M. Meade, and R. Edwards, 2007: Effective storm-relative helicity and bulk shear in supercell thunderstorm environments. *Wea. Forecasting*, **22**, 102-115.

- Trapp, R. J., D. M. Wheatley, N. T. Atkins, R. W. Przybylinski, and R. Wolf, 2006: Buyer beware: Some words of caution on the use of severe wind reports in postevent assessment and research. *Wea. Forecasting*, **21**, 408-415.
- Trapp, R. J., S. A. Tessendorf, E. S. Godfrey, and H. E. Brooks, 2005a: Tornadoes from squall lines and bow echoes. Part I: climatological distribution. *Wea. Forecasting*, **20**, 23-34.
- Trapp, R. J., G. J. Stumpf, and K. L. Manross, 2005b: A reassessment of the percentage of tornadic mesocyclones. *Wea. Forecasting*, **20**, 680-687.
- U. S. Department of Commerce, 2008: Storm Data, **50** (2). [Available from National Climatic Data Center, Asheville, NC 28801.]
- Weiss, S. J., J.A. Hart and P.R. Janish, 2002: An examination of severe thunderstorm wind report climatology: 1970-1999. Preprints, *21st Conf. Severe Local Storms*, San Antonio, TX, Amer. Meteor. Soc., 446-449.

7. FIGURES

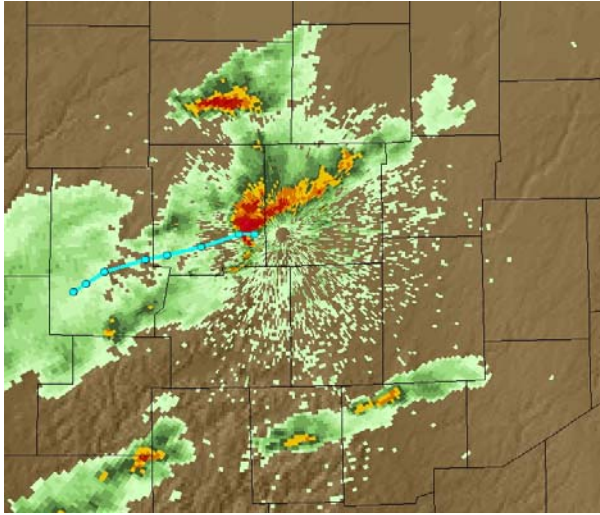


Fig. 1 Supercell points (blue circles) at volume scan times and supercell track (blue line) with KIND (Indianapolis, Indiana) single site 0.5 degree base reflectivity radar data.

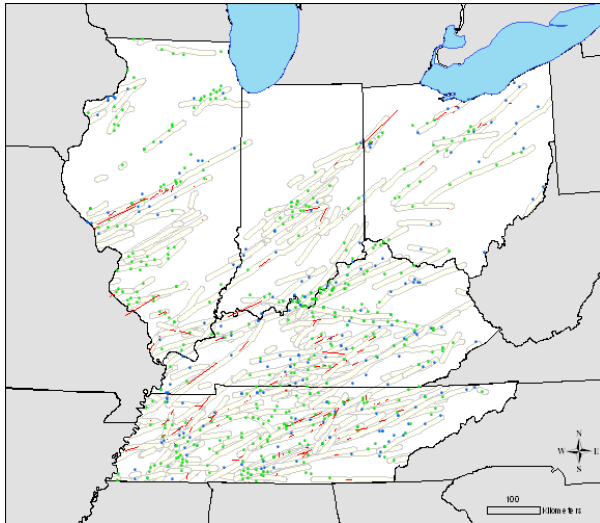


Fig. 2. Locations of supercell swaths (5 km radius), and supercell severe reports (tornadoes-red), (hail-green), (wind-blue) during the 1995-2006 cool seasons. Red segments denote longer-track tornadoes. Some reports are overlaid on other reports.

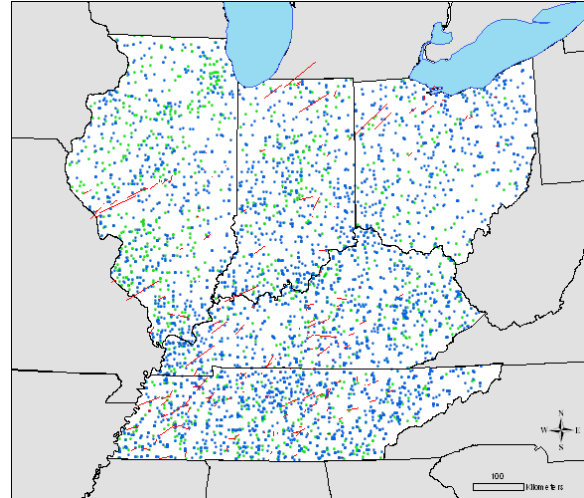


Fig. 3. Same as Fig. 2 except all severe reports locations (tornadoes-red), (hail-green), and (wind-blue) during the 1995-2006 cool seasons. Some reports are overlaid on other reports.

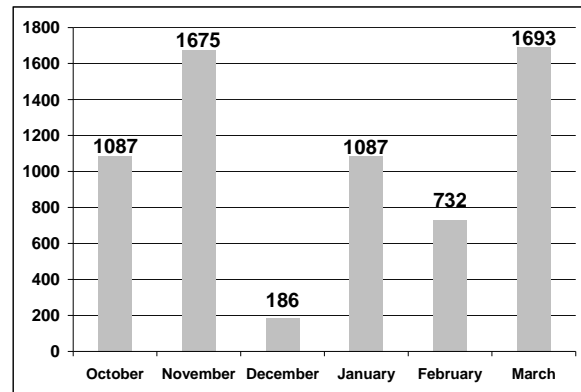


Fig. 4. Total cool season severe report (tornadoes, hail, and wind) count by month.

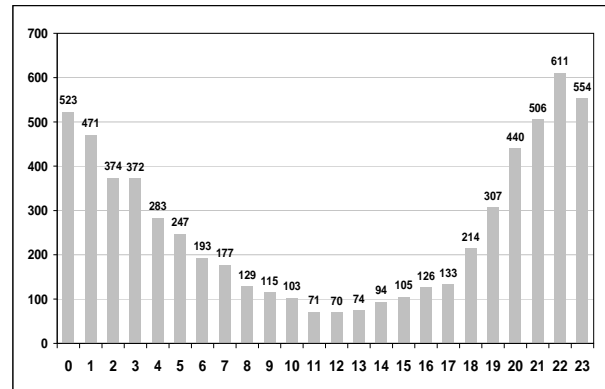


Fig. 5. Total cool season severe reports (tornadoes, hail, and wind) distribution count by time (UTC).

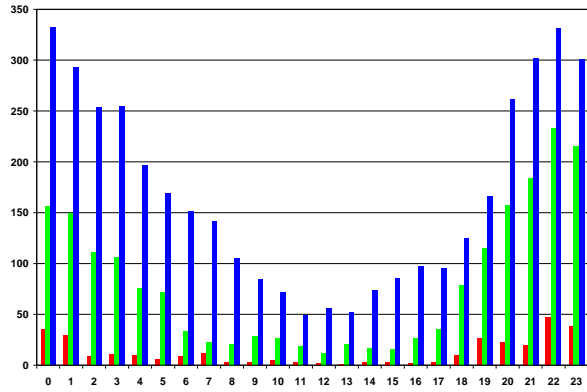


Fig. 6. Severe reports distribution by time (UTC) stratified by report type (tornadoes-red, wind-blue, hail-green).

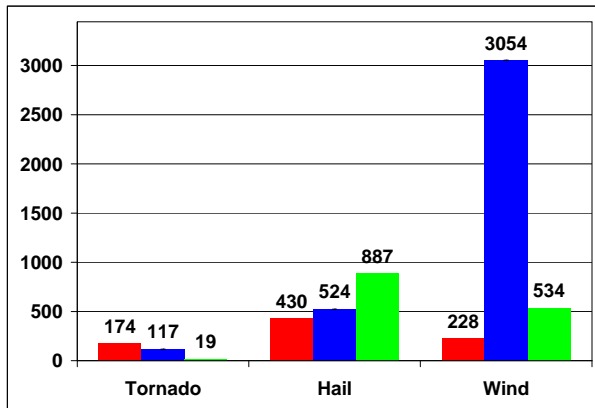


Fig. 7. Severe report (tornado, hail, wind) count by convective mode (supercell-red, QLCS-blue, single/multicell-green).

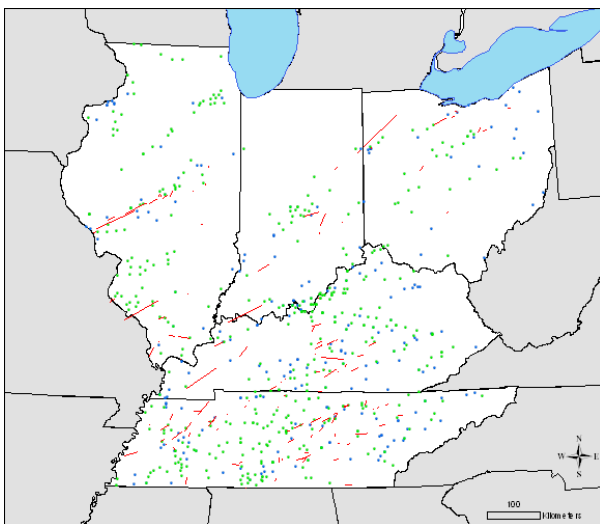


Fig. 8. Same report nomenclature as Fig. 3. except locations of supercell severe reports during the 1995-2006 cool season.

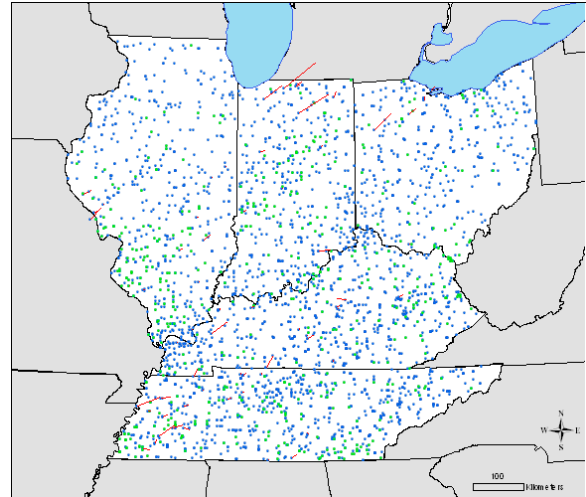


Fig. 9. Similar to Fig. 8 except for locations of QLCS severe reports.

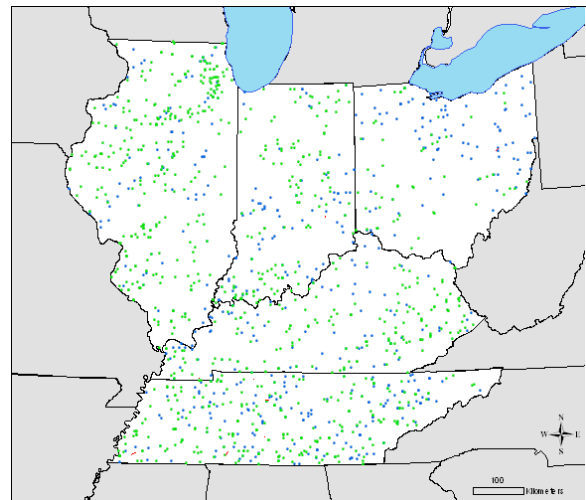


Fig. 10. Similar to Fig. 8 except for locations of (other) severe reports.

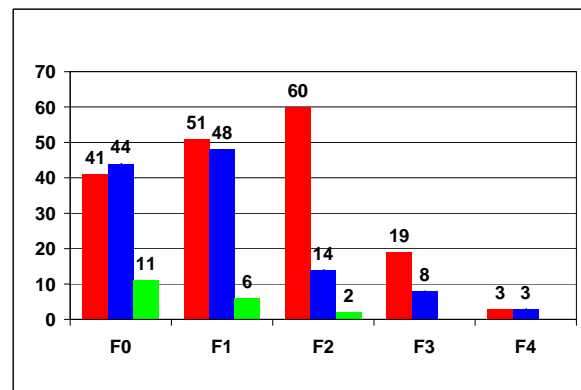


Fig. 11. Tornadoes by F-scale (supercell-red, QLCS-blue, other -green). There were no F5 tornadoes in this dataset.

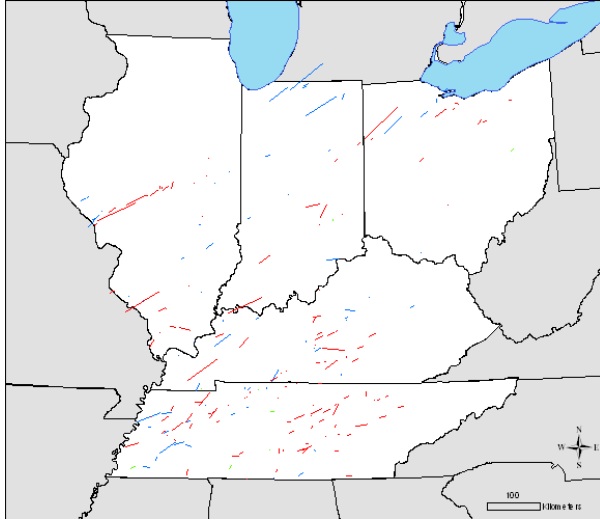


Fig. 12. Tornadoes by mode (supercell-red, QLCS-blue, other-green).

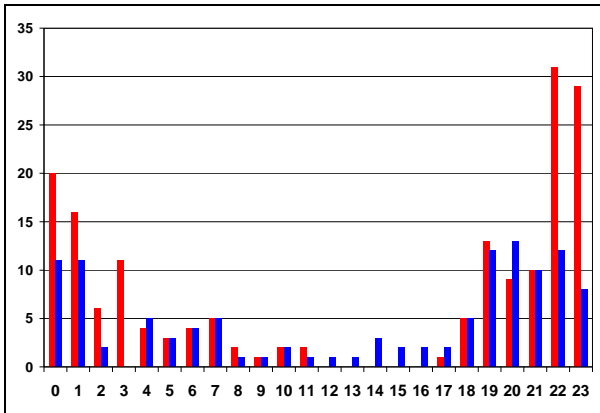


Fig. 13. Tornado distribution by time (UTC) (supercell-red, QLCS-blue).

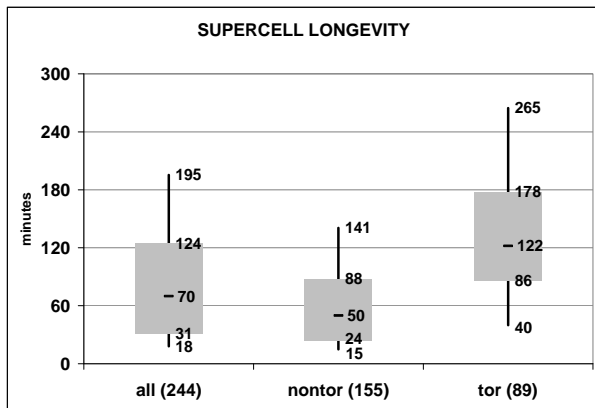


Fig. 14. Box and Whiskers plot of supercell longevity (minutes) for all supercells (244), nontornadic supercells (nontor, 155), and tornadic supercells (tor, 89). The shaded box covers the 25th-75th percentiles, the whiskers extend to the 10th and 90th percentiles, and

the median values are marked by the heavy horizontal line within each shaded box.

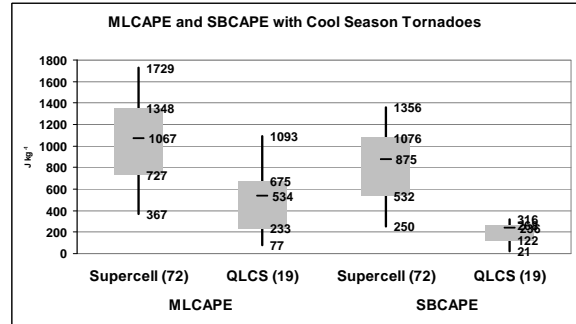


Fig. 15. Box and Whiskers plot of MLCAPE ($J kg^{-1}$) and SBCAPE ($J kg^{-1}$) for severe report grid hours for supercell tornado (72) and QLCS (19) tornado. The shaded box covers the 25th-75th percentiles, the whiskers extend to the 10th and 90th percentiles, and the median values are marked by the heavy horizontal line within each shaded box.

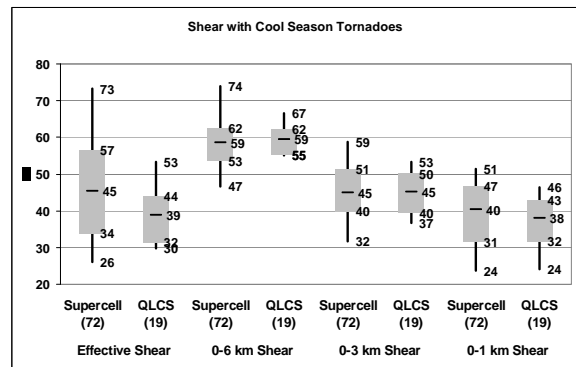


Fig. 16 Same as in Fig 15 except for effective bulk shear, 0-6 km shear, 0-3 km shear, and 0-1 km shear (kts) (AGL).

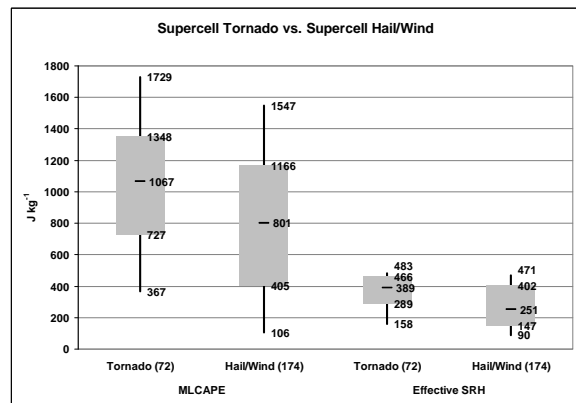


Fig. 17. Box and Whiskers plot of 100mb MLCAPE ($J kg^{-1}$) and Effective SRH ($m^2 s^{-2}$) for supercell tornadoes and supercell severe hail/wind grid hour

environments. Effective SRH (m^2s^{-2}) estimated via the Bunker's et al. (2000) storm motion algorithm.

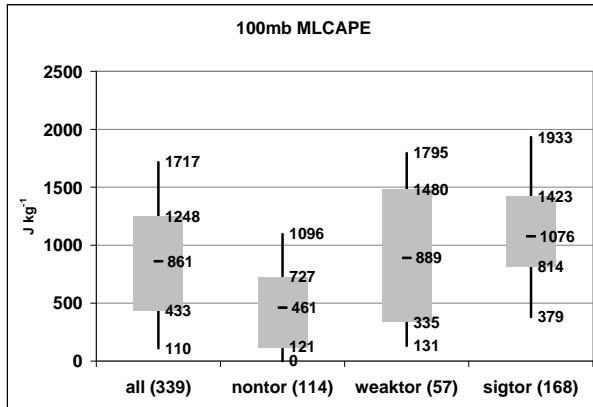


Fig. 18 Box and whiskers plot of MLCAPE (J kg^{-1}) for supercell grid hours for all supercells (339), non-tornadic supercells (nontor, 114), weakly tornadic supercells (weaktor, 57) and significantly tornadic supercells (sigtor, 168). The shaded box covers the 25th-75th percentiles, the whiskers extend to the 10th and 90th percentiles, and the median values are marked by the heavy horizontal line within each shaded box.

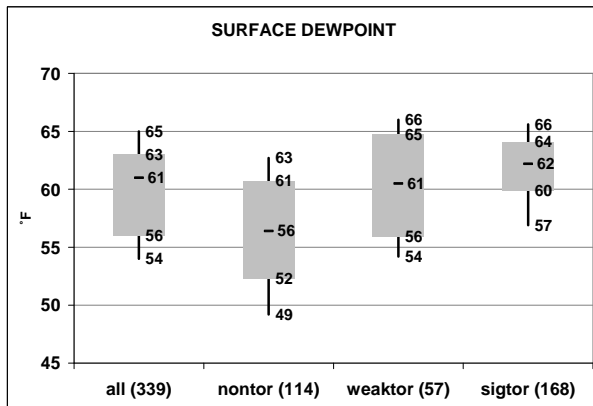


Fig. 19 Same as in Fig 18 except for surface dewpoint ($^{\circ}\text{F}$).

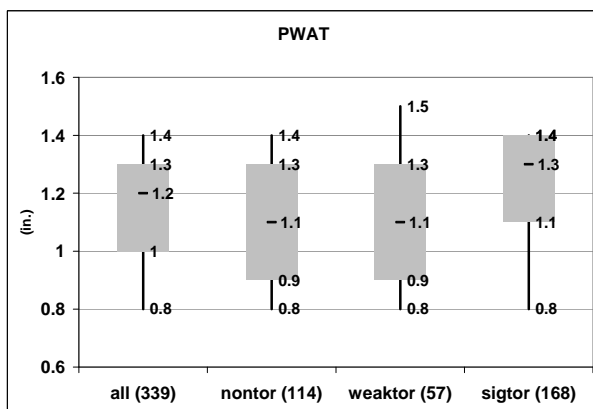


Fig. 20 Same as in Fig 18 except for precipitable water (in.).

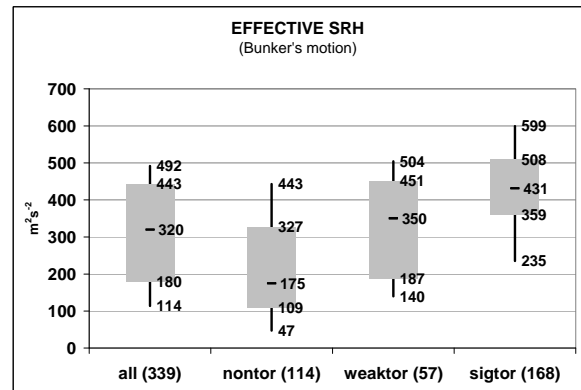


Fig. 21 Box and whiskers plot (same conventions as in Fig 18) except for Effective SRH (m^2s^{-2}) estimated via the Bunker's et al. (2000) storm motion algorithm for all four storm groups.

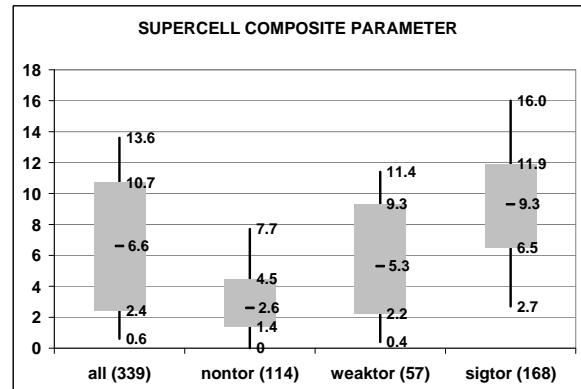


Fig. 22 Same as in Fig 21 except for Supercell Composite Parameter.

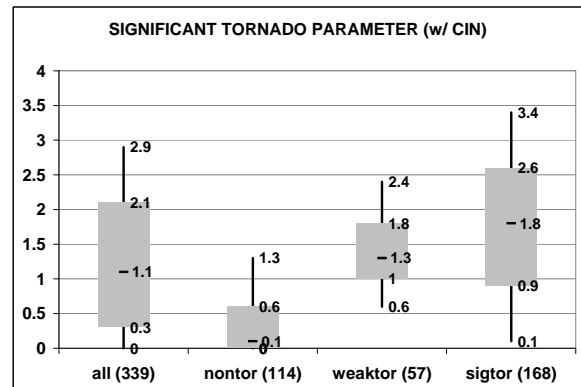


Fig. 23 Same as in Fig 21 except for Significant Tornado Parameter with CIN calculation.